Chiral Chemistry

Science Exploration

Open Access Research Article

Enantioselectivity synthesis of isoquinolin-1-one derivatives with C–N axial chirality via cobalt-catalyzed oxidative formal (4+2) cycloaddition: Light or not

Liang-Neng Wang[1], Yue-Liu-Ting Fu[1], Chun-Yan Liao[1], Wen-Jing Xiao[1,2,3,*], Liang-Qiu Lu[1,2,4,*]

[1]Hubei Engineering Research Center for Photochemistry and Technology, Engineering Research Centre of Photoenergy Utilization for Pollution Control and Carbon Reduction, Ministry of Education, College of Chemistry, Central China Normal University,Wuhan 430079, Hubei, China.
[2]Wuhan Institute of Photochemistry and Technology, Wuhan 430082, Hubei, China.
[3]State Key Laboratory of Organometallic Chemistry, Shanghai Institute of Organic Chemistry, Chinese Academy of Sciences, Shanghai 200032, China.
[4]School of Chemistry and Chemical Engineering, Henan Normal University, Xinxiang 453007, Henan, China.

***Correspondence to:** Liang-Qiu Lu, Hubei Engineering Research Center for Photochemistry and Technology, Engineering Research Centre of Photoenergy Utilization for Pollution Control and Carbon Reduction, Ministry of Education, College of Chemistry, Central China Normal University, Wuhan 430079, Hubei, China. E-mail: luliangqiu@ccnu.edu.cn

Received: December 08, 2025 **Accepted:** January 22, 2026 **Published:** January 28, 2026

Cite this article: Wang LN, Fu YLT, Liao CY, Xiao WJ, Lu LQ. Enantioselectivity synthesis of isoquinolin-1-one derivatives with C–N axial chirality via cobalt-catalyzed oxidative formal (4+2) cycloaddition: Light or not. Chiral Chem. 2026;2:202513. https://doi.org/10.70401/cc.2026.0012

Abstract

Developing mild and sustainable strategies for the synthesis of complex molecules is a pivotal yet challenging goal in modern synthesis. While cobalt catalysis offers a sustainable alternative to noble metals, achieving such transformations at room temperature remains elusive. Herein, we report a cobalt-catalyzed aerobic oxidative asymmetric formal cycloaddition involving C(sp^2)–H bond activation of benzamides with unactivated alkynes at room temperature using air as the oxidant. For challenging low-activity substrates, reaction efficiency is enhanced via a photoinduced catalytic cycle. Mechanistic and substrate scope studies indicate that substrate reactivity is influenced by electronic and steric effects.

Keywords: Axial chirality, cobalt catalysis, asymmetric C–H activation, aerobic oxidation, visible light

1. Introduction

Constructing molecular complexity with high efficiency under mild and environmentally friendly conditions is a central pursuit in synthetic chemistry[1,2]. Transition-metal-catalyzed oxidative C–H functionalization stands as a direct route for this purpose[3,4], yet it often depends on stoichiometric oxidants, such as Ag(I), Mn(III), oxone, or organic peroxides, to regenerate the active catalyst (Figure 1a). Replacing these oxidants with molecular oxygen represents a major step toward green synthesis[5-7]. Taking this further, the use of air is even more attractive due to its low cost, safety, and ready availability[8-10]. However, catalytic asymmetric reactions using air[11,12], particularly those proceeding efficiently at room temperature, are exceedingly rare, with only isolated reports for Ir[13], Ru[14,15], and Cu[16,17] systems. Therefore, the development of general catalytic methodologies that operate with air under ambient conditions remains a formidable and standing challenge.

Transition-metal-catalyzed asymmetric C–H functionalization has emerged as a direct and powerful strategy for constructing chiral molecules[18-20]. Among the various metals explored, earth-abundant and low-toxicity cobalt has demonstrated unique reactivity in C–H activation[21-24]. Since Yoshikai's seminal 2014 report on the cobalt-catalyzed enantioselective C(sp^2)–H intramolecular hydroacylation[25], significant advances have been witnessed in enantioselective cobalt catalysis. They are enabled by diverse chiral ligand systems, including phosphines[26,27], carboxylic acids[28-30], cyclopentadienyl ligands[31,32], and *N*-heterocyclic carbenes[33]. Notably, salicyloxazoline (Salox)-based ligands, originally developed by Bolm, have recently emerged as a privileged scaffold in this field (Figure 1b)[34]. While these systems have achieved substantial progress in enantioselective C(sp^2)–H functionalization[35-40], they

typically rely on stoichiometric oxidants and often require elevated temperatures. A critical step toward sustainability was taken by Niu in 2022[41], who successfully utilized oxygen gas to re-oxidize Co(I) to Co(III) in an asymmetric C–H activation, albeit under heating. Subsequently, photoirradiation strategies by Shi[42,43], Ackermann[44,45], Sundararaju[46], and Baidya[47] have demonstrated that light can activate O_2 for this oxidation, enabling transformations like indole dearomatization. More recently, Sundararaju[48] reported an elegant room-temperature, air-activated strategy for the construction of distal 1,3-C–N diaxes using indole-containing active alkynes. Inspired by these works, we questioned whether the catalytic cycle in asymmetric cobalt-catalyzed C–H activation could be driven by air at room temperature using non-activated alkynes. We hypothesized that coordinating an electron-rich ligand could lower the oxidation potential of the low-valent cobalt intermediate, facilitating its re-oxidation by air without external energy input (Figure 1c). Herein, building on our longstanding interest in photoinduced asymmetric cobalt catalysis[49-53], we report an efficient, cobalt-catalyzed aerobic oxidative enantioselective annulation of C(sp^2)–H bonds using air as the sole oxidant at ambient temperature, which is compatible with a variety of non-deactivated alkynes. Indeed, we found that the catalytic cycle can be augmented by photoinduced oxygen activation for less reactive alkynes and benzamides.

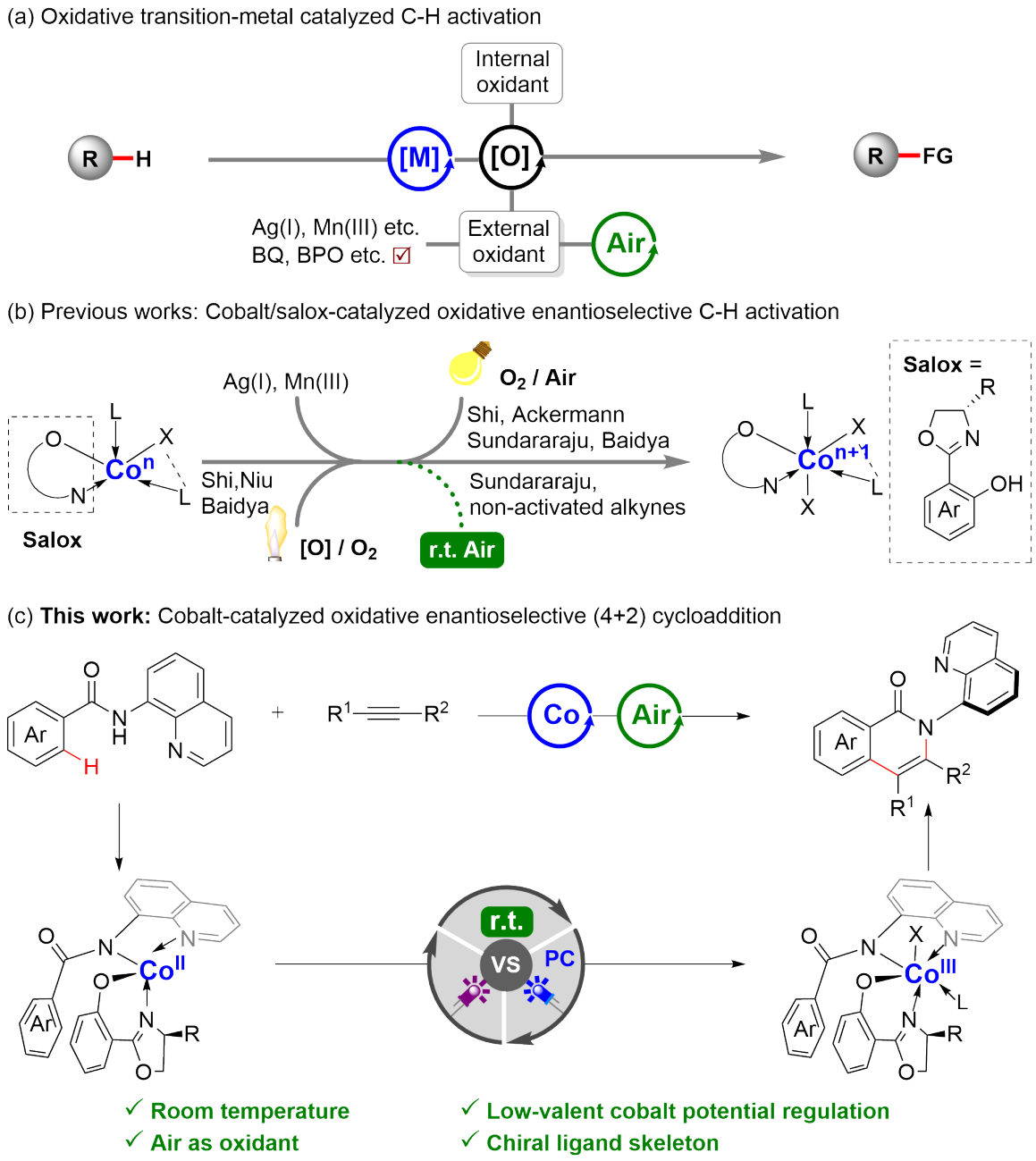

Figure 1. Design plan: cobalt-catalyzed oxidative enantioselective formal (4+2) cycloaddition.

2. Experimental/Methods

Under air, $Co(NO_3)_2·6H_2O$ (0.02 mmol, 5.82 mg), **L4** (0.015 mmol, 8.08 mg), and 1,1,1,3,3,3-hexafluoro-2-propanol (HFIP, 2 mL) were added to a 10 mL vial. After stirring at room temperature (rt) for 2 h, corresponding substrate **1** (0.2 mmol), alkyne **2** (0.3 mmol), **PC5** (1.64 mg, 0.004 mmol), and PivONa (49.9 mg, 0.4 mmol) were added to the resulting mixture. The mixture was stirred at rt under 5 W blue light-emitting diodes (LEDs) for approximately 48 h. The concentrated reaction residue was purified by flash column chromatography on silica gel with petroleum ether/ethyl acetate (3:1-1.5:1) as eluent to give the corresponding product **3**.

3. Results and Discussion

Initially, we investigated the reaction of 4-methyl-*N*-(quinolin-8-yl)benzamide **1a** with diphenylacetylene **2a** as the model substrates (Table 1). Preliminary screening revealed that the reaction conducted in 1,1,1,3,3,3-hexafluoro-2-propanol (HFIP) with $Co(NO_3)_2·6H_2O$ as the catalyst provided the product **3aa** in 46% yield and 90% ee (Tables S1 and S2 in Supporting Information). Notably, most alcoholic solvents exhibit relatively high yields and enantioselectivity, likely attributable to noncovalent interactions with the cobalt catalyst or salox ligand[48]. We then identified the optimal photocatalyst (**PC**) (Table 1, entries 1-5). Upon replacing the photocatalyst with **PC5** and irradiating with a 5 W blue LED, the yield increased significantly to 86%, while the enantioselectivity slightly decreased to 89% ee. Moreover, we found that atmospheric oxygen can also act as the terminal oxidant under otherwise identical conditions, resulting in almost consistent outcomes (Table 1, entry 6). Next, a series of chiral salox ligands was tested (Table 1, entries 7-11). A benzyl (**L2**) or indene skeleton (**L3**) on the oxazoline moiety dramatically reduced the enantioselectivity. The salox ligand with a methoxy substituent at the 5-position of the phenolic hydroxyl (**L4**) gave encouraging enantioselectivities of up to 95% ee and yields of 94%. Electron-withdrawing 5-CF_3-substituted (**L5**) and electron-donating 6-OMe-substituted (**L6**) salox ligands may reduce the stability of the monoanionic bidentate coordinating pattern. Surprisingly, the same product yield was achieved under control conditions: without **PC5** under purple LEDs (Entry 12) and neither light nor **PC5** (Entry 13). We then performed a preliminary substrate scope investigation. Substrates bearing different substituents (**3ba**, **3ga**, **3ka** in Table 1) showed markedly different reactivities under the three condition sets: (1) no light and no **PC5**, (2) purple LEDs without **PC5**, and (3) blue LEDs with **PC5**. These results clearly demonstrate that the necessity of photochemical conditions for this transformation depends critically on the electronic nature and the position of the substituents in the amide substrates **1**.

Subsequently, a series of mechanistic experiments was carried out to rationalize the way photocatalysis works and to understand the explicit role of the light (Figure 2). First, H/D exchange experiments were performed with **1b**/D_2O in the absence of both alkynes, **PC5** and light, and it was found that the recovered **1b** was hardly deuterated at the *ortho*-positions of the phenyl ring (Figure 2a). This indicates that the cleavage of the C−H bond is irreversible. Second, the parallel kinetic isotope effect (KIE, $\mathbf{k_H/k_D}$ = 1.2) was evaluated, suggesting that C−H bond cleavage may not be involved in the rate-determining step (Figure 2b). Third, employing the cobaltacycle intermediate **[Co]-1** in a stoichiometric reaction with alkynes can give the desired cycloadduct **3ga** in 93% yield with 99% ee (Figure 2c). Under catalytic conditions, **[Co]-1** delivered **3ga** in 96% yield with 89% ee (Figure 2d). Both experiments indicate that the chiral ligand chelated Co(III) species **[Co]-1** might be involved in the catalytic cycle. The structure of **[Co]-1** was confirmed by X-ray diffraction (CCDC: 2489953).

To gain a more mechanistic understanding, we performed electron paramagnetic resonance (EPR) studies with 2,2,6,6-tetramethylpiperidin-4-one (**4-Oxo-TEMP**) as a singlet oxygen ($^1O_2$) trapping agent (Figure 2e)[54,55]. When **4-Oxo-TEMP** was added under condition B, a triple peak signal was observed after 10 min of 5 W purple LEDs irradiation, with g = 2.0056 and A_N = 1.58 mT (purple trace). Such a spectrum was in good agreement with the simulated EPR spectrum of piperidine *N*-oxygen radical **4-Oxo-TEMPO** (blue trace). This result provides evidence for the existence of singlet oxygen ($^1O_2$). Next, the three sets of unsubstituted (**1b**), 4-Br-substituted (**1g**), and 2-Br-substituted (**1k**) benzamide derivatives were selected as models to explore their optical and electrical properties in this system. First, addition of 2 equiv of DMA decreased the yield from 51% to 29% under 5 W purple LEDs. In contrast, no significant change was observed under conditions of no light or 5 W blue LEDs and **PC5**, supporting that $^1O_2$ is generated under purple LEDs (Figure 2f). Then, to elucidate the role of light in promoting the oxidation of low-valent cobalt by oxygen, we performed a series of control experiments using the 4-Br-substituted benzamide derivative **1g** as the model substrate (Figure 2g). In the absence of both the photocatalyst **PC5** and light, the reaction afforded only 25% yield after 15 h. While $Mn(OAc)_3·2H_2O$ (2 equiv) gave a 78% yield, light irradiation increased it to 54%, and the extending the time (40 h) further increased to 95%, supporting our hypothesis that light facilitates aerobic oxidation, albeit less effectively than the stoichiometric oxidant. Next, we measured the UV/Vis spectra for each component of the system and the different mixtures using 2-Br-substituted benzamide derivatives (**1k**) as substrate (Figure 2h). The solutions containing the mixture of **[Co]**+**L4**, **[Co]**+**1k**, and **[Co]**+**L4**+**1k** had a distinct absorption in the visible light region. Subsequent fluorescence quenching experiments showed that **[Co]**+**L4**+**1k** had a more significant quenching effect on the **PC5** as compared to **[Co]**+**1k** and **[Co]**+**L4** (Figure 2i). In addition, detailed cyclic voltammetry tests were conducted to investigate the effects of ligand **L4** and benzamide derivatives (Figure 2j). A comparison of the oxidation potentials of **[Co]** (E_{onset}(**[Co]**) = 2.09 V vs. SCE in HFIP) and **[Co]**+**L4** (E_{onset}(**[Co]**+**L4**) = 1.19 V vs. SCE in HFIP) revealed that the addition of ligand could reduce the oxidation potentials of **[Co]**. Whereas the introduction of benzamide derivatives further altered the oxidation potential of the in situ generated **[Co]**+**L4**+**1** complexes. Comparison of **[Co]**+**L4**+**1b** (E_{onset}(**[Co]**+**L4**+**1b**) = 0.90 V vs. SCE in HFIP) and **[Co]**+**L4**+**1g** (E_{onset}(**[Co]**+**L4**+**1g**) = 1.01 V vs. SCE in

HFIP) showed that electron-withdrawing substitution of the benzamide derivative leads to an increase in the oxidation potential of the **[Co]+L4+1** complex. The further increase in the oxidation potential of **[Co]+L4+1k** (E_{onest}(**[Co]+L4+1k**) = 1.21 V vs. SCE in HFIP) indicated that the *ortho*-substituted substrate weakens the coordination of the benzamide derivative to the cobalt center due to steric hindrance, resulting in a further increase in the oxidation potential of the **[Co]+L4+1** complex.

Table 1. Optimization of reaction conditions.[a]

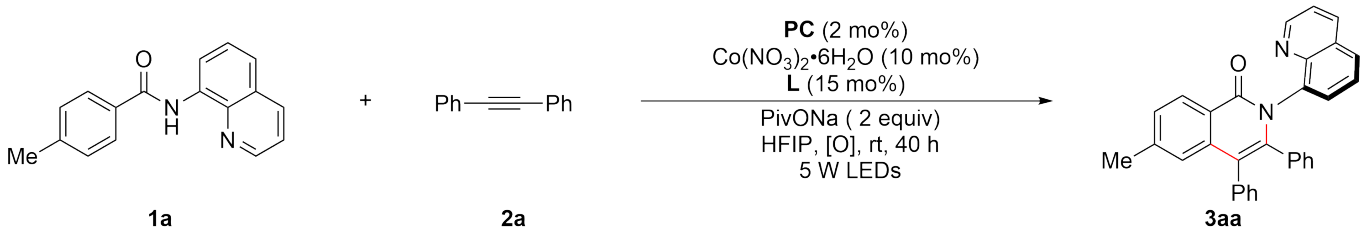

1a **2a** **3aa**

Entry	PC	Light	Oxidant	L	Yield (%)	ee (%)
1	**PC1**[b]	5 W white LEDs	O_2	**L1**	46	90
2	**PC2**[b]	5 W white LEDs	O_2	**L1**	51	89
3	**PC3**	5 W white LEDs	O_2	**L1**	14	85
4	**PC4**	5 W blue LEDs	O_2	**L1**	30	85
5	**PC5**	5 W blue LEDs	O_2	**L1**	86	89
6	**PC5**	5 W blue LEDs	Air	**L1**	85	89
7	**PC5**	5 W blue LEDs	Air	**L2**	95	61
8	**PC5**	5 W blue LEDs	Air	**L3**	85	67
9	**PC5**	5 W blue LEDs	Air	**L4**	94	95
10	**PC5**	5 W blue LEDs	Air	**L5**	87	82
11	**PC5**	5 W blue LEDs	Air	**L6**	67	75
12	-	5 W purple LEDs	Air	**L4**	94	96
13	-	No light	Air	**L4**	93	96

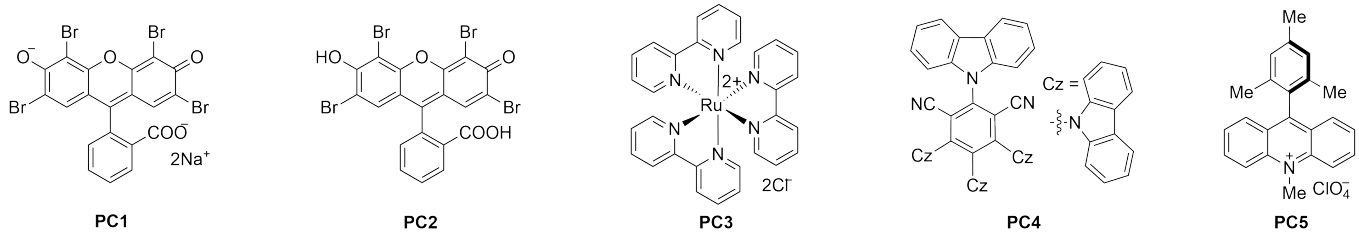

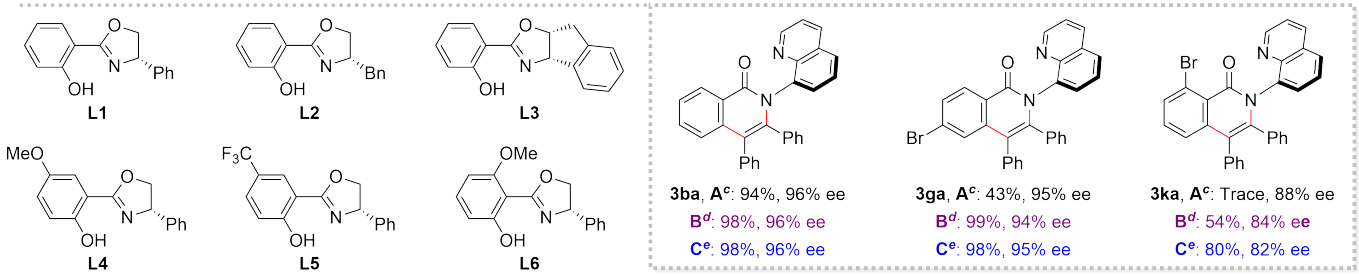

3ba, **A**[c]: 94%, 96% ee
B[d]: 98%, 96% ee
C[e]: 98%, 96% ee

3ga, **A**[c]: 43%, 95% ee
B[d]: 99%, 94% ee
C[e]: 98%, 95% ee

3ka, **A**[c]: Trace, 88% ee
B[d]: 54%, 84% ee
C[e]: 80%, 82% ee

[a]: **1a** (0.1 mmol), **2a** (0.15 1mmol), **PC** (2 mol%), $Co(NO_3)_2·6H_2O$ (10 mol%), **L** (15 mol%), PivONa (2 equiv) in HFIP (1 mL) under O_2 at rt for 40 h. Yields were determined using ^{1}H NMR spectroscopy with 1,3,5-trimethoxybenzene as an internal standard. All the ee values in this work were determined by chiral HPLC analysis of purified products; [b]: Using **PC** (10 mol%); [c]: Without light and **PC5**; [d]: Under 5 W purple LEDs instead of 5 W blue LEDs, without **PC5**; [e]: Using 5 W blue LEDs and **PC5**. LED: light-emitting diode; HFIP: 1,1,1,3,3,3-hexafluoro-2-propanol; PC: photocatalyst; NMR: nuclear magnetic resonance.

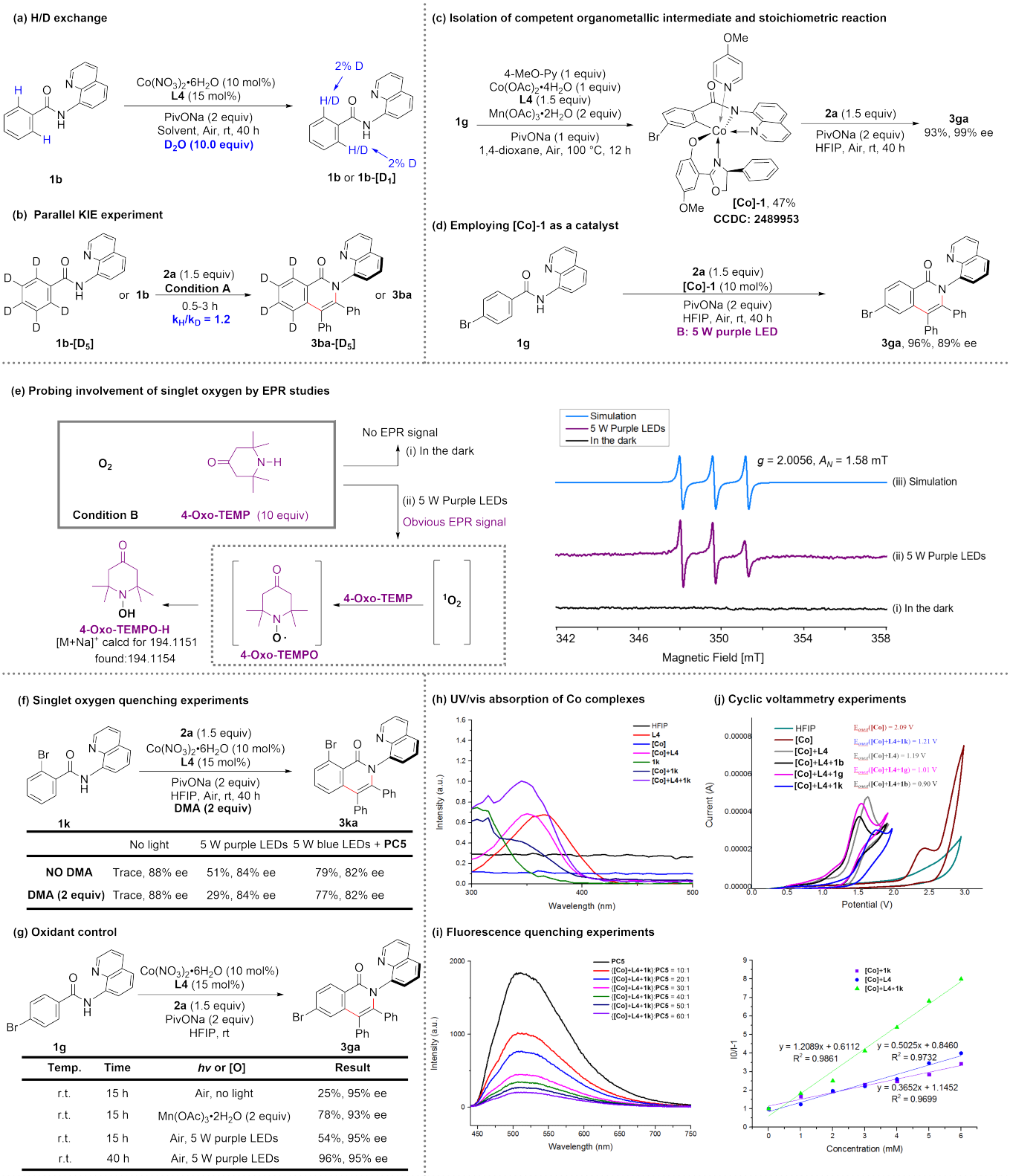

Figure 2. Mechanistic experiments. **[Co]**, $Co(NO_3)_2{\cdot}H_2O$. **DMA**, 9,10-dimethylanthracene.

Combined with the three sets of conditions and detailed experimental results required in the reaction, three distinct mechanistic pathways were proposed in the process of oxidative regeneration of cobalt(III) **Int-2** (Figure 3). In the conditions without both **PC** and light, the reaction undergoes path a: the cobalt(II) intermediate **Int-1** was oxidized directly by oxygen to the cobalt(III) intermediate **Int-2**, releasing the superoxide anion $O_2^{\bullet-}$. In the conditions of 5 W purple LEDs without **PC**, the reaction undergoes path b: the ground state oxygen ($^3O_2$) was excited by purple light to afford the singlet oxygen ($^1O_2$), and then the cobalt(II) intermediate **Int-1** was oxidized

by the singlet oxygen ($^1O_2$) to the cobalt(III) intermediate **Int-2**, accompanied by the release of superoxide anion $O_2^{\bullet-}$. In the conditions of 5 W blue LEDs and **PC**, the reaction undergoes path c: the ground state **PC** reaches an excited state (**PC***) under irradiation with blue LED, which is subsequently quenched by cobalt (II) **Int-1** in a reductive process via a SET pathway and forms $PC^{\bullet-}$. The oxidation of $PC^{\bullet-}$ by oxygen delivers the ground state **PC** and the superoxide anion $O_2^{\bullet-}$.

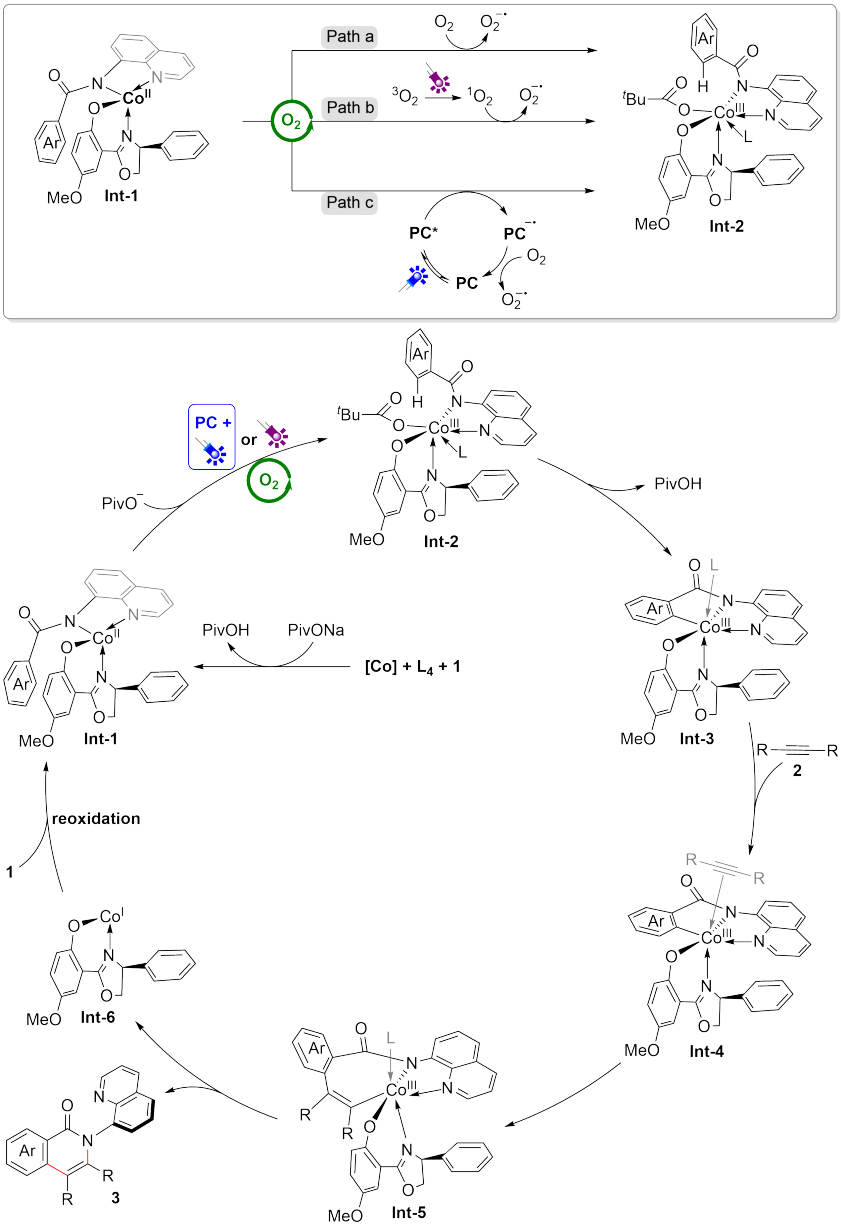

Figure 3. Possible Mechanism.

Based on the mechanistic studies and related literature, a plausible mechanism was proposed (Figure 3). Firstly, cobalt(II) salt coordinates with **L4** and substrate **1** to generate the cobalt(II) intermediate **Int-1**, which is oxidized to the cobalt(III) **Int-2** by oxygen in the air. Notably, this process may need to be facilitated by direct photoexcitation and photoredox catalysis, considering the different electrical properties and steric hindrances of the substrates. Subsequently, carboxylate-assisted C–H activation led to the five-membered cobaltacycle intermediate **Int-3**, which undergoes ligand exchange with alkynes **2** to give the intermediate **Int-4**. Then, the migratory insertion of C–Co(III) bond of alkynes **2** affords the seven-membered cobaltacycle intermediate **Int-5**. Finally, the reductive elimination of **Int-5** leads to chiral product **3**, releasing the cobalt(I) intermediate **Int-6**, which could be easily re-oxidized to the cobalt(II) intermediate **Int-1** under aerobic conditions.

After determining the optimal reaction conditions and plausible mechanism, we began to investigate the substrate scope of this asymmetric oxidative [4+2] cycloaddition under three different reaction conditions (Figure 4). Electron-donating substituted diarylacetylenes (**3ab**, **3ac**) gave the desired products with reduced yields under the conditions without both **PC5** and light, and the

irradiation with a 5 W purple LEDs was necessary in order to ensure a good yield. Electron-withdrawing substituted diarylacetylenes (**3ad**-**3ag**) and diheteroarylacetylene (**3ah**) had low yields without both **PC5** and light. However, irradiation with a 5 W purple LEDs improved the yield, while a 5 W blue LEDs and **PC5** gave better results. Unfortunately, 4-Br-substituted diarylacetylene (**3af**) afforded lower yields under all three sets of conditions, likely due to the poor solubility of **2f** in HFIP. Nevertheless, light still produced a measurable yield enhancement. Alkyl alkynes (**3ai**, **3aj**) with low site resistance also gave good yields under the conditions without both **PC5** and light, which can be attributed to the fact that the alkynes act as weak electron-rich ligand to facilitate the oxidative regeneration of low-valent cobalt intermediates[56]. Asymmetric di-substituted alkynes (**3ak**, **3al**) showed moderate yields under conditions without both **PC5** and light, although prop-1-yn-1-ylbenzene (**3ak**) was poorly regionally selective. When mono-substituted aryl (**3am**), heteroaryl (**3an**), cyclohexenyl (**3ao**), and diphenylphosphinyl (**3ap**, **3aq**) acetylenes were used as substrates, irradiation with a 5 W purple LEDs always enhanced the yield, and the yield was further improved under the condition of a 5 W blue LEDs and **PC5**. Remarkably, 2-thiophene acetylene (**3an**) only maintained a moderate yield. This low reactivity could be partially explained by sulfur-induced inactivation of the cobalt catalyst[57].

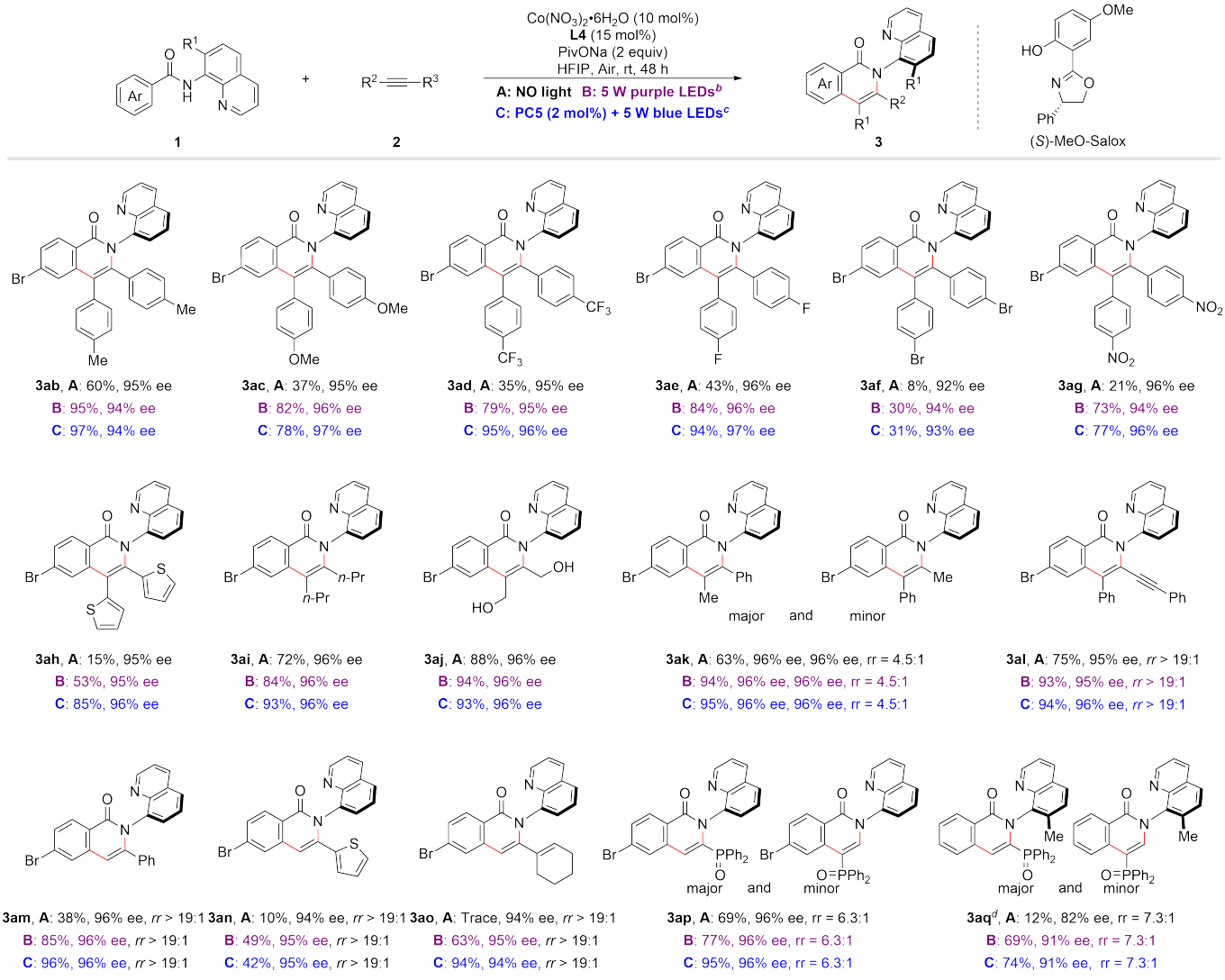

Figure 4. The scope of alkynes. [a]: **1** (0.2 mmol), **2** (0.3 mmol), $Co(NO_3)_2$•H_2O (10 mol%), **L4** (15 mol%), PivONa (2 equiv) in HFIP (2 mL) under air at rt for 48 h, isolated yields; [b]: Under 5 W purple LED; [c]: Using **PC5** (2 mol%), 5 W blue LED; [d]: Using $Co(NO_3)_2$·H_2O (30 mol%), **L4** (45 mol%). LED: light-emitting diode; HFIP: 1,1,1,3,3,3-hexafluoro-2-propanol.

We next turned our attention to determining the scope of arylamides that are amenable to asymmetric cyclization reaction under the three sets of conditions (Figure 5). A range of amide groups containing electron-neutral or -rich substituents at the *para*-position, such as Me, H, OMe, could be employed as suitable substrates, and the corresponding products (**3aa**-**3ca**) were all produced in good to excellent yields (82-98%) with high enantioselectivity (96-97% ee) under the three sets of conditions. However, the analogous reaction with electron-deficient substituents at the *para*-position, such as CO_2Me (**3da**), SO_2Me (**3ea**), CN (**3fa**), Br (**3ga**), and I (**3ia**), was less effective under the conditions without both **PC5** and light, and irradiation with a 5 W purple LEDs was needed to ensure good

yields. *Ortho*-substituted Br, Cl, 1-naphthyl, and 3,5-/2,4-di-substituted (**3ja**-**3na**) benzamide derivatives did not react or had only trace yields without both **PC5** and light. Again, the yield can be increased by irradiation with a 5 W purple LED, and the replacement of a 5 W blue LEDs and **PC5** led to better results. Remarkably, 2-thienylamide (**3oa**) and the introduction of an electron-rich group (Me, **3ia**) at the 2-position of the benzamide are well tolerated under the three sets of conditions. Heterocyclic amides, including 3-thienyl (**3pa**), 2-furanyl (**3qa**), 3-furanyl (**3ra**), and *ortho*-substituted pyridine (**3sa**) were subsequently reacted, with inferior results obtained without both **PC5** and light, but irradiation with a 5 W purple LEDs often resulted in significantly enhanced yields. Benzamides bearing electron-deficient (F, Cl, Br, I), or electron-rich (Me, OMe) substituents in the *meta*-position reacted efficiently with **2a** to give the corresponding product **3ta**□**3ya** in good to excellent yields (78-96% yield) and high enantioselectivity (90-96% ee) under the three sets of conditions. The regioselectivity (C2 or C6) was entirely determined by the size of the steric hindrance of the substituent group. The steric hindrance may weaken the coordination between *N*-atom and the cobalt center and reduce the electron density of the low-valent cobalt intermediate. Additionally, the 2-position (**3za**) or 7-position(**3aaa**) methyl substitution on quinoline also leads to a decrease in enantioselectivity. The absolute stereochemistry of **3aa** was established by X-ray diffraction (CCDC: 2416014).

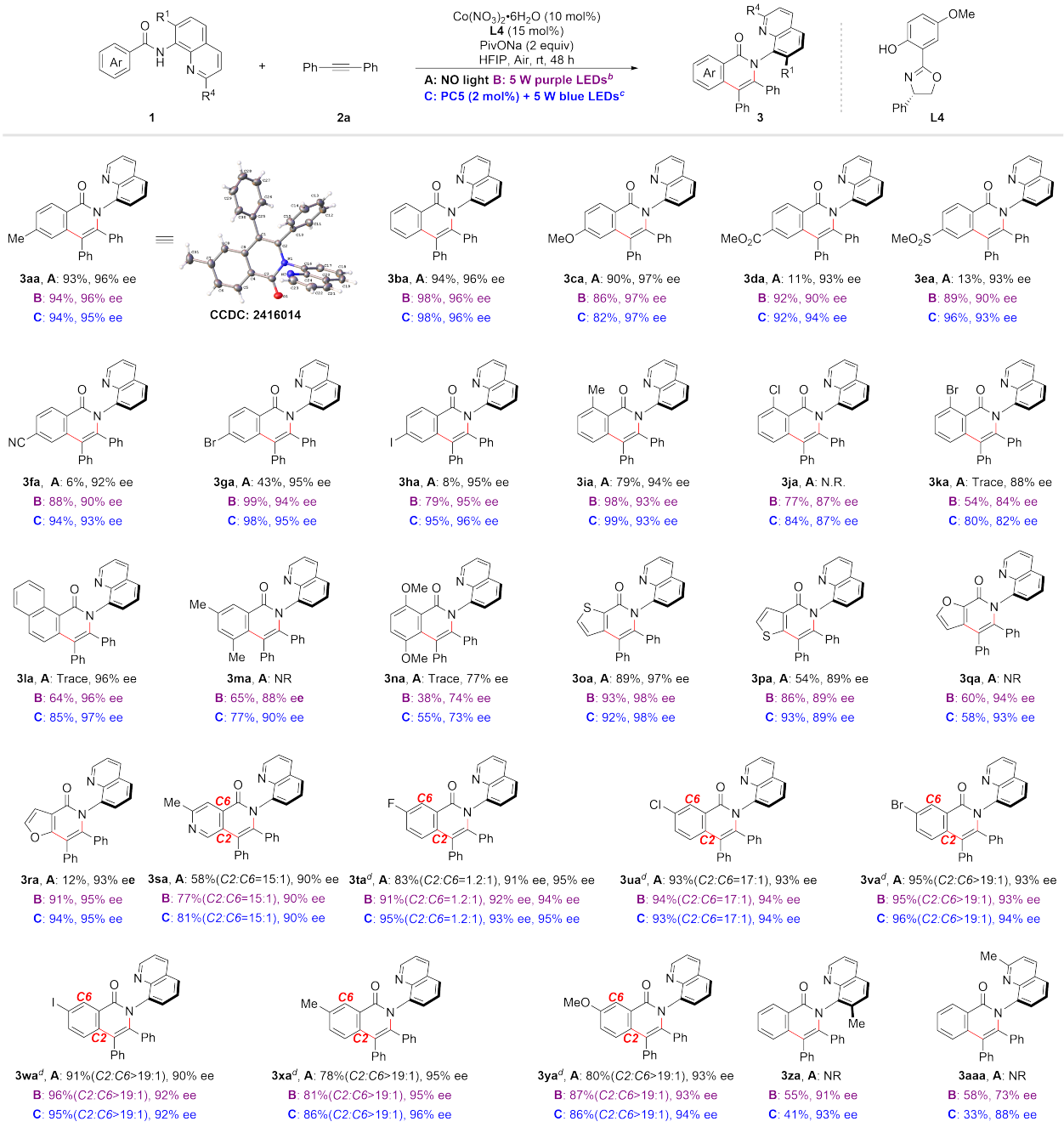

Figure 5. The scope of arylamides. [a]: **1** (0.2 mmol), **2** (0.3 mmol), $Co(NO_3)_2{\cdot}H_2O$ (10 mol%), **L4** (15 mol%), PivONa (2 equiv) in HFIP (2 mL) under air at rt for 48 h, isolated yields; [b]: under 5 W purple LED; [c]: Using **PC5** (2 mol%), 5 W blue LED; [d]: 36 h. LED: light-emitting diode; HFIP: 1,1,1,3,3,3-hexafluoro-2-propanol.

Product **3aq**-major could be smoothly transformed to C–N axially chiral monophosphine compound **4** with high enantioselectivity by using $HSiCl_3$ (Figure 6a). Notably, the compound **4** could act as a potential chiral ligand for the palladium-catalyzed asymmetric Tsuji-Trost reaction, providing the desired product **7** in 78% yield with 45% ee (Figure 6b).

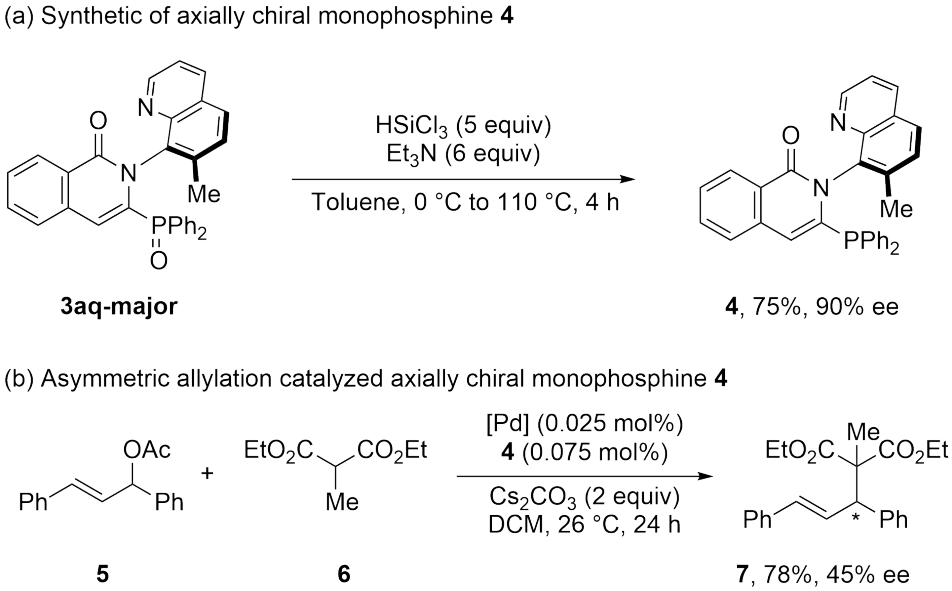

Figure 6. Synthetic application.

4. Conclusion

In summary, we have developed a Co-catalyzed asymmetric aerobic oxidative C(sp^2)–H bond activation/[4+2] cycloaddition. The reactions proceed under room temperature with air as an oxidant, and provided an efficient and highly enantioselective method for the assembly of axially chiral isoquinolinones. Light irradiation can increase the yield of lowly active substrates by activating oxygen. Preliminary experiments indicate that this axially chiral skeleton is a promising chiral ligand for Pd-catalyzed asymmetric reactions. Substrate studies and mechanistic experiments reveal a correlation between substrate activity and its substituent electrical properties and steric hindrance. We believe that this work provides an unprecedentedly mild and sustainable new strategy for transition metal catalyzed asymmetric aerobic oxidation.

Supplementary materials

The supplementary material for this article is available at: Supplementary materials.

Declarations

Acknowledgement

We thank Prof. Jia-Rong Chen, Prof. Zhihan Zhang, and many other group members for helpful discussions.

Authors contributions

Wang LN: Investigation, writing-original draft.
Fu YLT: Writing-review & editing.
Liao CY: Investigation, Resources.
Xiao WJ: Methodology, writing-review & editing.
Lu LQ: Conceptualization, methodology, writing-review & editing.

Conflicts of interest

The authors declare that they have no conflicts of interest.

Ethical approval

Not applicable.

Consent to participate

Not applicable.

Consent to publication

Not applicable.

Data availability statement

Please change this part to: The data supporting this article have been included as part of the Supplementary Information. CCDC 2489953 and 2416014 contain the supplementary crystallographic data for this paper. These data can be obtained free of charge via www.ccdc.cam.ac.uk/data_request/cif, or by emailing data_request@ccdc.cam.ac.uk, or by contacting The Cambridge Crystallographic Data Centre, 12 Union Road, Cambridge CB2 1EZ, UK; fax: +44 1223 336033.

Funding

This work was supported by the National Natural Science Foundation of China (Grant Nos. 92256301, 22471089, and 22271113), and the National Key R & D Program of China (Grant Nos. 2023YFA1507203 and 2024YFA1509700).

References

1. Zhang G, Bian C, Lei A. Advances in visible-light-mediated oxidative coupling reactions. Chin J Catal. 2015;36(9):1428-1439. [DOI]
2. Cannalire R, Pelliccia S, Sancineto L, Novellino E, Tron GC, Giustiniano M. Visible light photocatalysis in the late-stage functionalization of pharmaceutically relevant compounds. Chem Soc Rev. 2021;50(2):766-897. [DOI]
3. Yang Y, Lan J, You J. Oxidative C–H/C–H coupling reactions between two (hetero)arenes. Chem Rev. 2017;117(13):8787-8863. [DOI]
4. Rogge T, Kaplaneris N, Chatani N, Kim J, Chang S, Punji B, et al. C–H activation. Nat Rev Methods Primers. 2021;1:43. [DOI]
5. Shi Z, Zhang C, Tang C, Jiao N. Recent advances in transition-metal catalyzed reactions using molecular oxygen as the oxidant. Chem Soc Rev. 2012;41(8):3381-3430. [DOI]
6. Bryliakov KP. Catalytic asymmetric oxygenations with the environmentally benign oxidants H_2O_2 and O_2. Chem Rev. 2017;117(17):11406-11459. [DOI]
7. Kananovich D, Elek GZ, Lopp M, Borovkov V. Aerobic oxidations in asymmetric synthesis: Catalytic strategies and recent developments. Front Chem. 2021;9:614944. [DOI]
8. Chen G, Shao P, Niu X, Wu LZ, Zhang T. Innovative and sustainable approaches to aerobic oxidation reactions for organics upgrading. CCS Chem. 2025;7(5):1272-1288. [DOI]
9. Sun X, Li X, Song S, Zhu Y, Liang YF, Jiao N. Mn-catalyzed highly efficient aerobic oxidative hydroxyazidation of olefins: A direct approach to β-azido alcohols. J Am Chem Soc. 2015;137(18):6059-6066. [DOI]
10. Yu Y, Xia Z, Wu Q, Liu D, Yu L, Xiao Y, et al. Direct synthesis of benzoxazinones via Cp*Co(III)-catalyzed C–H activation and annulation of sulfoxonium ylides with dioxazolones. Chin Chem Lett. 2021;32(3):1263-1266. [DOI]
11. Uchida T, Katsuki T. Green asymmetric oxidation using air as oxidant. J Synth Org Chem Jpn. 2013;71(11):1126-1135. [DOI]
12. Goicoechea L, Losada P, Mascareñas JL, Gulías M. Palladium-catalyzed enantioselective C–H arylations and alkenylations of 2-aminobiaryls with atmospheric air as the sole oxidant. Angew Chem Int Ed. 2025;64(20):e202425512. [DOI]
13. Ikariya T, Kuwata S, Kayaki Y. Aerobic oxidation with bifunctional molecular catalysts. Pure Appl Chem. 2010;82(7):1471-1483. [DOI]
14. Koya S, Nishioka Y, Mizoguchi H, Uchida T, Katsuki T. Asymmetric epoxidation of conjugated olefins with dioxygen. Angew Chem Int Ed. 2012;51(33):8243-8246. [DOI]
15. Mizoguchi H, Uchida T, Katsuki T. Ruthenium-catalyzed oxidative kinetic resolution of unactivated and activated secondary alcohols with air as the hydrogen acceptor at room temperature. Angew Chem Int Ed. 2014;53(12):3178-3182. [DOI]
16. Maji B, Yamamoto H. Asymmetric synthesis of tertiary α-hydroxy phosphonic acid derivatives under aerobic oxidation conditions. Synlett. 2015;26(11):1528-1532. [DOI]
17. Verdhi LK, Fridman N, Szpilman AM. Copper- and chiral nitroxide-catalyzed oxidative kinetic resolution of axially chiral N-arylpyrroles. Org Lett. 2022;24(28):5078-5083. [DOI]
18. Newton CG, Wang SG, Oliveira CC, Cramer N. Catalytic enantioselective transformations involving C–H bond cleavage by transition-metal complexes. Chem Rev. 2017;117(13):8908-8976. [DOI]
19. Achar TK, Maiti S, Jana S, Maiti D. Transition-metal-catalyzed enantioselective C(sp^2)–H bond functionalization. ACS Catal. 2020;10(23):13748-13793. [DOI]
20. Wang Q, Liu CX, Gu Q, You SL. Chiral CpxRh complexes for C–H functionalization reactions. Sci Bull. 2021;66(3):210-213. [DOI]
21. Yoshikai N. Cobalt-catalyzed asymmetric C–H functionalization. In: Maiti D, editor. Handbook of C–H Functionalization. Weinheim: Wiley-

VCH; 2022. p. 1-19. [DOI]
22. Gao K, Yoshikai N. Low-valent cobalt catalysis: New opportunities for C–H functionalization. Acc Chem Res. 2014;47(4):1208-1219. [DOI]
23. Moselage M, Li J, Ackermann L. Cobalt-catalyzed C–H activation. ACS Catal. 2016;6(2):498-525. [DOI]
24. Zheng Y, Zheng C, Gu Q, You SL. Enantioselective C–H functionalization reactions enabled by cobalt catalysis. Chem Catal. 2022;2(11):2965-2985. [DOI]
25. Yang J, Yoshikai N. Cobalt-catalyzed enantioselective intramolecular hydroacylation of ketones and olefins. J Am Chem Soc. 2014;136(48):16748-16751. [DOI]
26. Whyte A, Torelli A, Mirabi B, Prieto L, Rodríguez JF, Lautens M. Cobalt-catalyzed enantioselective hydroarylation of 1,6-enynes. J Am Chem Soc. 2020;142(20):9510-9517. [DOI]
27. Ghosh KK, RajanBabu TV. Ligand effects in carboxylic ester- and aldehyde-assisted β-C–H activation in regiodivergent and enantioselective cycloisomerization–hydroalkenylation and cycloisomerization–hydroarylation, and [2+2+2]-cycloadditions of 1,6-enynes. J Am Chem Soc. 2024;146(27):18753-18770. [DOI]
28. Pesciaioli F, Dhawa U, Oliveira JCA, Yin R, John M, Ackermann L. Enantioselective cobalt(III)-catalyzed C–H activation enabled by chiral carboxylic acid cooperation. Angew Chem Int Ed. 2018;57(47):15425-15429. [DOI]
29. Fukagawa S, Kato Y, Tanaka R, Kojima M, Yoshino T, Matsunaga S. Enantioselective C(sp^3)–H amidation of thioamides catalyzed by a cobalt(III)/chiral carboxylic acid hybrid system. Angew Chem Int Ed. 2019;58(4):1153-1157. [DOI]
30. Liu YH, Xie PP, Liu L, Fan J, Zhang ZZ, Hong X, et al. Cp*Co(III)-catalyzed enantioselective hydroarylation of unactivated terminal alkenes via C–H activation. J Am Chem Soc. 2021;143(45):19112-19120. [DOI]
31. Ozols K, Jang YS, Cramer N. Chiral cyclopentadienyl cobalt(III) complexes enable highly enantioselective 3d-metal-catalyzed C–H functionalizations. J Am Chem Soc. 2019;141(14):5675-5680. [DOI]
32. Ozols K, Onodera S, Woźniak Ł, Cramer N. Cobalt(III)-catalyzed enantioselective intermolecular carboamination by C–H functionalization. Angew Chem Int Ed. 2021;60(2):655-659. [DOI]
33. Jacob N, Zaid Y, Oliveira JCA, Ackermann L, Wencel-Delord J. Cobalt-catalyzed enantioselective C–H arylation of indoles. J Am Chem Soc. 2022;144(2):798-806. [DOI]
34. Bolm C, Weickhardt K, Zehnder M, Ranff T. Synthesis of optically active bis(2-oxazolines): crystal structure of a 1,2-bis(2-oxazolinyl)benzene·$ZnCl_2$ complex. Chem Ber. 1991;124(5):1173-1180. [DOI]
35. Garai B, Das A, Vineet Kumar D, Sundararaju B. Enantioselective C–H bond functionalization under Co(III)-catalysis. Chem Commun. 2024;60:3354-3369. [DOI]
36. Yao QJ, Shi BF. Cobalt(III)-catalyzed enantioselective C–H functionalization: ligand innovation and reaction development. Acc Chem Res. 2025;58(6):971-990. [DOI]
37. Yang T, Zhang Y, Dou Y, Yang D, Niu JL. Earth-abundant cobalt-catalyzed enantioselective C–H functionalizations. Sci China Chem. 2025. [DOI]
38. Yao QJ, Chen JH, Song H, Huang FR, Shi BF. Cobalt/Salox-catalyzed enantioselective C–H functionalization of arylphosphinamides. Angew Chem Int Ed. 2022;61(25):e202202892. [DOI]
39. von Münchow T, Dana S, Xu Y, Yuan B, Ackermann L. Enantioselective electrochemical cobalt-catalyzed aryl C–H activation reactions. Science. 2023;379:1036-1042. [DOI]
40. Wu X, Tian Q, Ge J, Liu Y, Li Z, Zhang J, et al. Cobalt-catalyzed regio-, diastereo-, and enantioselective C–H annulation of aminoquinoline amides with internal alkynes for the construction of diaxes. Chin J Chem. 2025;43(20):2669-2676. [DOI]
41. Si XJ, Yang D, Sun MC, Wei D, Song MP, Niu JL. Atroposelective isoquinolinone synthesis through cobalt-catalysed C–H activation and annulation. Nat Synth. 2022;1(9):709-718. [DOI]
42. Teng MY, Liu DY, Mao SY, Wu X, Chen JH, Zhong MY, et al. Asymmetric dearomatization of indoles through cobalt-catalyzed enantioselective C–H functionalization enabled by photocatalysis. Angew Chem Int Ed. 2024;63(40):e202407640. [DOI]
43. Qian PF, Zhou G, Hu JH, Wang BJ, Jiang AL, Zhou T, et al. Asymmetric synthesis of chiral calix[4]arenes with both inherent and axial chirality via cobalt-catalyzed enantioselective intermolecular C–H annulation. Angew Chem Int Ed. 2024;63(52):e202412459. [DOI]
44. Xu Y, Lin Y, Homölle SL, Oliveira JCA, Ackermann L. Enantioselective cobaltaphotoredox-catalyzed C–H activation. J Am Chem Soc. 2024;146(34):24105-24113. [DOI]
45. Xu Y, Pandit NK, Meraviglia S, Boos P, Stark PAM, Surke M, et al. Stereocontrolled construction of multi-chiral [2.2]paracyclophanes via cobaltaphotoredox dual catalysis. ACS Catal. 2025;15(13):11716-11725. [DOI]
46. Das A, Kumaran S, Sankar RHS, Premkumar JR, Sundararaju B. A dual cobalt-photoredox catalytic approach for asymmetric dearomatization of indoles with aryl amides via C–H activation. Angew Chem Int Ed. 2024;63(40):e202406195. [DOI]
47. Koner M, Ballav N, Varma AJ, Ghosh S, Mondal T, Kuniyil R, et al. Multifaceted photocatalysis enables cobalt-catalyzed enantioselective C–H activation and APEX reaction for C–N axially chiral molecules. Chem Sci. 2025;16(41):19296-19303. [DOI]
48. Das A, Kumaran S, Maity P, Premkumar JR, Sundararaju B. Cobalt-catalyzed enantioselective and diastereodivergent construction of C–N atropisomers. J Am Chem Soc. 2025;147(30):26226-26237. [DOI]
49. Lu FD, Chen J, Jiang X, Chen JR, Lu LQ, Xiao WJ. Recent advances in transition-metal-catalysed asymmetric coupling reactions with light intervention. Chem Soc Rev. 2021;50(22):12808-12843. [DOI]
50. Jiang X, Han X, Lu FD, Lu LQ, Zuo Z, Xiao WJ. Stereocontrol strategies in asymmetric organic photochemical synthesis. CCS Chem. 2025;7(6):1567-1602. [DOI]

51. Zhang K, Lu LQ, Jia Y, Wang Y, Lu FD, Pan F, et al. Exploration of chiral cobalt catalyst for visible-light-induced enantioselective radical conjugate addition. Angew Chem Int Ed. 2019;58(38):13375-13379. [DOI]
52. Jiang X, Xiong W, Deng S, Lu FD, Jia Y, Yang Q, et al. Construction of axial chirality via asymmetric radical trapping by cobalt under visible light. Nat Catal. 2022;5(9):788-797. [DOI]
53. He XK, Lu LQ, Yuan BR, Luo JL, Cheng Y, Xiao WJ. Desymmetrization–addition reaction of cyclopropenes to imines via synergistic photoredox and cobalt catalysis. J Am Chem Soc. 2024;146(28):18892-18898. [DOI]
54. Rosenthal I, Krishna CM, Yang GC, Kondo T, Riesz P. A new approach for EPR detection of hydroxyl radicals by reaction with sterically hindered cyclic amines and oxygen. FEBS Lett. 1987;222(1):75-78. [DOI]
55. Wandt J, Jakes P, Granwehr J, Gasteiger HA, Eichel RA. Singlet oxygen formation during the charging process of an aprotic lithium–oxygen battery. Angew Chem Int Ed. 2016;128(24):7006-7009. [DOI]
56. Winternheimer DJ, Merlic CA. Alkoxydienes via copper-promoted couplings: Utilizing an alkyne effect. Org Lett. 2010;12(11):2508-2510. [DOI]
57. Nishida M, Fujii S, Aoki T, Hayakawa Y, Muramatsu H, Morita T. Synthesis and polymerization of ethynylthiophenes and ethynylfurans containing trifluoromethyl groups. J Fluorine Chem. 1990;46(3):445-459. [DOI]

Publisher's Note